PHOTOB-2022-0111-ver9-daCruz_1P
Type: research-article

Photobiomodulation, Photomedicine, and Laser Surgery
Volume 41, Number 4, 2023

Pp. 1–7
DOI: 10.1089/photob.2022.0111

Original Research

Open camera or QR reader and scan code to access this article and other resources online.

Optical Properties of Human Skin Phototypes and Their Correlation with Individual Angle Typology

AU1 ▶ AU2 ▶ Luismar Barbosa da Cruz Junior,[1] Carlos Eduardo Girasol,[2] Pedro Soler Coltro,[3] Rinaldo Roberto de Jesus Guirro,[2] and Luciano Bachmann[1]

AU4 ▶ **Abstract**

Objective: This study aims to correlate human skin phototypes with complete optical characterization (absorption, scattering, effective attenuation, optical penetration, and albedo coefficients) based on individual typology angle (ITA) values and colorimetric parameters.
Methods: A colorimeter was used to group 12, fresh, ex vivo human skin samples according to their phototype; the CIELAB color scale and ITA values were employed. An integrating sphere system and the inverse adding–doubling algorithm were applied during optical characterization, conducted from 500 to 1300 nm.
Results: On the basis of ITA values and their classification, the skin samples were separated into six groups: two intermediates, two tan, and two brown. In the visible range, for lower ITA values (darker skins), the absorption and effective attenuation coefficient parameters increased, whereas the albedo and depth penetration parameters decreased. In the infrared region, all the phototypes had similar parameters. The scattering coefficient was similar for all the samples and did not change with ITA values.
Conclusions: ITA analysis, a quantitative method, showed that the human skin tissue's optical properties and pigmentation colors were highly correlated.

Keywords: individual typology angle, optical characterization, spectroscopy, human skin

Introduction

Understanding how light propagates in biological tissues is extremely important for diagnostic and therapeutic methods.[1,2] This knowledge may improve patients' and physicians' safety and increase comprehension of medical treatments to help develop new therapeutic methods.[3] Light propagation in a turbid medium, which is the case of most biological tissues, can be described by the radiative transport equation[4] or transport equations[5] through four optical parameters: absorption (μ_a) and scattering (μ_s) coefficients, refractive index (n), and anisotropy factor (g).

Several articles have described the optical characterization of ex vivo human skin samples[6–9]; however, most of them have analyzed stored or *postmortem* samples between a day and 1 week after patient's surgery or death. Genina et al.[10] showed that depending on the storage process, the optical properties may change. In addition, skin phototypes are not usually considered.

When skin phototypes are taken into consideration, the Fitzpatrick scale is often used to categorize samples according to the melanin response to sunlight. Nevertheless, grouping skins by phototypes in one large batch on the basis of the Fitzpatrick scale could induce a subjective evaluation.[11] Indeed, other factors can change the tissue optical properties, including age,[12] chromophore concentration,[8] lesions,[13] and exposure to the sun.[14]

To reduce subjectivity when grouping human skins by phototypes, the individual typology angle (ITA) can be employed. Chardon et al.[15] initially proposed using ITA to establish skin color categories by applying the $L^*a^*b^*$ scale measured through a spectrometer or colorimeter. Bino's

AU3 ▶ [1]Laboratory of Phobiophysics, Department of Physics, University of São Paulo, Ribeirão Preto, Brazil.
[2]Laboratory of Physiotherapeutic Resources, Department of Health Sciences, University of São Paulo, Ribeirão Preto, Brazil.
[3]Division of Plastic Surgery, Ribeirão Preto Medical School, University of São Paulo, Ribeirão Preto, Brazil.

study[16] showed that ITA is directly correlated with constitutive skin pigmentation, and Zonios et al.[17] found a linear relationship between ITA and melanin concentration. However, no relationship with optical properties has been described so far.

There are several medical and technological applications where knowledge about the optical information of different skin phototypes can be relevant for improving treatment and device sensitivity. Some examples include tattoo removal[1] and low-level laser therapy.[2] Recently, Sjoding et al.[3] suggested that pulse oximeter devices could lead to errors and be less accurate for people with darker skin pigmentation.

Therefore, a quantitative and reproductive method is needed for better understanding how skin phototypes influence photonic procedures. In this sense, this study aims to correlate the skin phototype with the respective optical properties in fresh ex vivo samples.

Materials and Methods

The optical properties of 12 fresh samples of ex vivo abdominal human skin were analyzed within 3 h after surgery and separated into 6 different groups according to their ITA values obtained by colorimetric measurements. All the donors were adult females aged between 36 and 65 years, and the measurements were performed on the skin after cleaning. An integrating sphere system was employed to measure diffuse reflectance and transmittance.

Then, the optical absorption (μ_a) and reduced scattering (μ'_s) coefficients were computed by the inverse adding–doubling (IAD) method. By using the experimental absorption and reduced scattering coefficients, the effective attenuation coefficient (μ_{eff}), depth penetration (δ), and albedo (a) values of the samples were calculated and correlated with ITA values.

Tissue samples

Tissue samples were obtained in association with the Plastic Surgery Division of Ribeirão Preto Medical School, University of São Paulo, after regular abdominoplasty surgery procedures for improving the body contour. All procedures were performed according to ethical standards and were approved by the Ethics Committee (ethics appreciation certificate 0630218.2.0000.5440 and approval number 3.275.034).

Human abdominal skin samples were obtained from different donors and grouped into six sets according to their ITA values. There were 12 skin tissue samples separated into group 1, $n=5$, intermediate, ITA = 32.7°; group 2, $n=2$, intermediate, ITA = 29.0°; group 3, $n=1$, tan, ITA = 22.4°; group 4, $n=2$, tan, ITA = 18.4°; group 5, $n=1$, brown, ITA = −4.2°; and group 6, $n=1$, brown, ITA = −13.5°.

All the skin tissue samples can be seen in Fig. 1. As a reference, groups 1 and 2 are Fitzpatrick type I or II, groups 3 and 4 are Fitzpatrick type III, group 5 is Fitzpatrick type IV, and group 6 is Fitzpatrick type V; however, there is no direct correlation between the Fitzpatrick scale and ITA values.[18]

Sample preparation for the optical measurement consisted of manually removing most of the fat, blood, and fluids from the collected samples to leave only intact dermis and epidermis. The measurements were performed within 3 h after the surgery, so sample freshness was maintained. Thickness ranged from 1.69 to 1.92 mm.

Colorimetry

A colorimeter (Delta Vista 450G; Delta Color, Brazil) was used to assess the $L^*a^*b^*$ scale, which uses a three-dimensional scale to describe all the colors perceived by human eyes. L^* describes brightness/luminance, while a^* describes green and red colors and b^* is related to blue and yellow colors. Measurements were carried out in triplicate; only the average was considered. Experimental values were used in Equation (1) to compute ITA and skin typology. To avoid experimental errors, a recalibration routine was performed before each measurement.

$$\text{ITA} = \frac{180}{\pi} \arctan\left(\frac{L^* - 50}{b^*}\right) \quad (1)$$

ITA, measured in degrees, was used to analyze sample pigmentation,[16] and classification was as follows: higher than 55° = very light, 55° to 41° = light, 41° to 28° = intermediate, 28° to 10° = tan, 10° to −30° = brown, and lower than −30° = dark.[15,16]

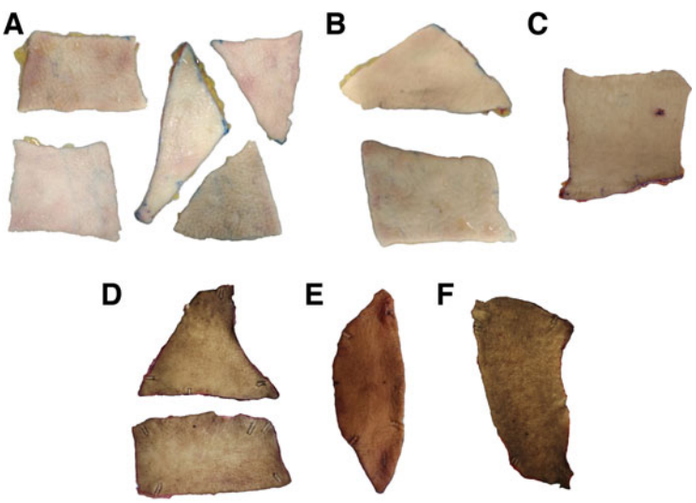

FIG. 1. Human skin samples grouped and categorized by ITA: **(A)** group 1 has five samples with mean ITA = 36.7 ± 0.6 and intermediate typology. **(B)** Group 2 has two samples with mean ITA = 29.0 ± 0.4 and intermediate typology. **(C)** Group 3 has one sample with ITA = 22.4 ± 1.0 and tan typology. **(D)** Group 4 has two samples with mean ITA = 18.4 ± 0.8 and tan typology. **(E)** Group 5 has one sample with ITA = −4.2 ± 0.9 and brown typology. **(F)** Group 6 has one sample with ITA = −13.5 ± 0.7 and brown typology. Only the background was removed. ITA, individual typology angle.

Optical system and data acquisition

AU5 ▶ 3D printed double integrating spheres with a sphere diameter of 150 mm, input and sample ports of 35 mm, detector port and baffle of 10 mm, and barium sulfate as the internal coating were employed. An SLS201 light source (Thorlabs) and two spectrometers—RPS900-R (International Light) for measurements from 500 to 950 nm and AU6 ▶ AVASPEC-NIR (Avantes, The Netherlands) for measurements from 950 to 1300 nm—were used. More details about the manufacturing and validation of this system can be seen in Cruz Junior's study.[19]

The IAD algorithm was employed to determine the optical absorption and reduced scattering coefficients. The IAD method consists in iteratively solving the transport equation for a layered semi-infinite medium with a known refractive index to compute $\boldsymbol{\mu_a}$ and $\boldsymbol{\mu'_s}$.[5] Information about the system is also required to compensate for light losses. Three experimental values must be supplied to the algorithm: experimental diffuse reflectance ($\boldsymbol{M_r}$) and transmittance ($\boldsymbol{M_t}$), according to Equations (2) and (3), and the anisotropy factor (g) as a corrective factor:

$$\boldsymbol{M_r} = \boldsymbol{R}_{\text{std}}\left(\frac{\boldsymbol{R}_{\text{sample}} - \boldsymbol{B_k}}{\boldsymbol{R}_{\text{source}} - \boldsymbol{B_k}}\right) \tag{2}$$

$$\boldsymbol{M_t} = \left(\frac{\boldsymbol{T}_{\text{sample}} - \boldsymbol{B_k}}{\boldsymbol{T}_{\text{source}} - \boldsymbol{B_k}}\right) \tag{3}$$

Where $\boldsymbol{R}_{\text{sample}}$ and $\boldsymbol{T}_{\text{sample}}$ are the experimental diffuse reflection and transmission of the sample, respectively; $\boldsymbol{R}_{\text{source}}$ and $\boldsymbol{T}_{\text{source}}$ are the source signal on the reflectance sphere and transmittance sphere, respectively; $\boldsymbol{R}_{\text{std}}$ is the standard reference reflectance; and $\boldsymbol{B_k}$ is the background noise.

More information about the algorithm and experimental procedure can be found in the IAD manual provided by Prahl.[20] For the samples, the anisotropy factor $\boldsymbol{g} = 0.9$ and refractive index $\boldsymbol{n} = 1.4$ were employed because these are the most common values for skin tissues.[8]

Optical evaluation

To describe a turbid medium optically, the refractive index (n), anisotropy factor (g), and absorption ($\boldsymbol{\mu_a}$) and scattering ($\boldsymbol{\mu_s}$) coefficients should be known.

Some properties may also be described as a combination of the previous parameters; for example, the reduced scattering ($\boldsymbol{\mu'_s}$) and effective attenuation ($\boldsymbol{\mu}_{\text{eff}}$) coefficients, depth penetration ($\boldsymbol{\delta}$), and albedo ($\boldsymbol{a}$), according to Equations (4)–(7):

$$\boldsymbol{\mu'_s} = (1 - \boldsymbol{g})\boldsymbol{\mu_s} \tag{4}$$

$$\boldsymbol{\mu_{eff}} = \sqrt{3\boldsymbol{\mu_a}(\boldsymbol{\mu'_s} + \boldsymbol{\mu_a})} \tag{5}$$

$$\delta = \frac{1}{\boldsymbol{\mu}_{\text{eff}}} \tag{6}$$

$$a = \frac{\boldsymbol{\mu'_s}}{\boldsymbol{\mu'_s} + \boldsymbol{\mu_a}} \tag{7}$$

$\boldsymbol{\mu'_s}$ considers the average scattering angle ($\boldsymbol{g} = \langle cos\ \theta \rangle$) as an isotropic correction of $\boldsymbol{\mu_s}$ in turbid samples; $\boldsymbol{\mu}_{\text{eff}}$ represents the absorption and scattering effects that reduce fluence; $\boldsymbol{\delta}$ indicates the depth where the light falls to $1/\boldsymbol{e}$ of its initial value after its first interaction with the medium, where $\boldsymbol{e}$ is the Euler number; and $\boldsymbol{a}$ indicates the portion of the attenuated light that is scattered.[8]

Since the scattering coefficient pattern decreases with increasing wavelength, a power law curve can be fitted according to Equation (8):

$$\boldsymbol{\mu'_s} = \boldsymbol{c}_1\left(\frac{\lambda}{500\text{ nm}}\right)^{-c_2} \tag{8}$$

where $\boldsymbol{c}_1$ and $\boldsymbol{c}_2$ are arbitrary model parameters for amplitude and scattering power, respectively, and the function is normalized by a reference wavelength (500 nm).

Results and Discussion

Colorimetric measures

The Fitzpatrick scale is a classification system commonly used to categorize skin tones based on their response to sun exposure, and ITA is the newest skin tone classification system that takes into account skin color using reliable spectroscopic measurements. The ITA system is more comprehensive and accurate in assessing an individual's skin tone, making it a better choice in situations where precise color matching is required, such as in the cosmetic industry, light-based treatments, and optical devices (e.g., optical oximeters).[21] Therefore, the Fitzpatrick scale can be changed to ITA in situations where more detailed and accurate skin tone classification is necessary.

By using the experimental L^* and b^* values of each sample, we obtained the ITA values through Equation (1) and grouped the samples according to their ITA values. The results can be seen in Table 1. ◀ T1

The $L^*a^*b^*$ results resembled the description presented in Alaluf's study.[22] We observed that skin samples with lighter classification, such as groups 1 and 2, generally had higher L^* and lower b^* values. The inverse was true for darker skin. We also noted that parameter a^* gradually increased for darker classifications, except for the sample in group 3, categorized as tan.

Some sample groups appeared to be visually similar in terms of color; however, the ITA measurements showed that the skin samples were different. For instance, group 1, with ITA of 32.7°, and group 2, with ITA of 29.0°, were categorized as intermediate types, but had ΔITA of 3.7°. Group 3, with ITA of 22.4°, and group 4, with ITA of 18.4°, were categorized as tan, but had ΔITA of 4.0°.

Table 1. Average and Standard Deviation for the $L^*A^*B^*$ Color Scale, Individual Typology Angle Values, and Skin Classification of the Six Abdominal Skin Sample Groups

Group	L*	a*	b*	*ITA (degrees)*	*Typology*
1	60.7 ± 1.2	3.9 ± 1.0	16.4 ± 2.0	32.7 ± 0.6	Intermediate
2	59.5 ± 0.2	5.0 ± 1.2	17.3 ± 0.5	29.0 ± 0.4	Intermediate
3	56.7 ± 1.0	9.5 ± 0.8	16.3 ± 1.6	22.4 ± 1.0	Tan
4	57.6 ± 1.2	6.1 ± 1.2	22.3 ± 1.8	18.4 ± 0.8	Tan
5	48.5 ± 1.6	8.4 ± 0.3	20.9 ± 0.1	–4.2 ± 0.9	Brown
6	44.8 ± 0.7	10.5 ± 0.5	21.7 ± 0.7	–13.5 ± 0.7	Brown

ITA, individual typology angle.

The opposite happened in samples with distant ITA values, but the same classification—group 5, with ITA of −4.2°, and group 6, with ITA of −13.5°, which had ΔITA of 9.3°, were still the brown type.

Absorption and reduced scattering coefficients

F2 ▶ Figure 2 shows the experimental absorption from 500 to 1300 nm and the reduced scattering coefficient wavelength dependence of the skin groups labeled by ITA values. The average values are shown in solid lines, and vertical bars correspond to the standard deviations.

The scattering coefficient decreased in most spectra in Fig. 2A, except for ITA = −13.5°. The low μ'_s for ITA = −13.5°, from 500 to 600 nm, was due to the high absorption F3 ▶ in this range, which decreased the albedo (Fig. 3B). The latter may not completely converge to the IAD algorithm.[5] However, μ_a in this sample seemed to be reliable.

Scattering was higher at 500 nm ($\sim 3\ mm^{-1}$) and lower at 1300 nm ($\sim 1.3\ mm^{-1}$). Bashkatov et al.[8] described that μ'_s decreases from 500 to 800 nm and stabilizes at higher wavelengths. We observed this behavior for all the skin samples included in this study, but in a lower wavelength range, from 500 to 650 nm. By using Equation (8), we performed a power law fit from the reduced scattering co- T2 ▶ efficient (Table 2) to compute coefficients c_1 and c_2. In this analysis, we did not consider μ'_s of group 6, with ITA of −13.5°, due to its abnormal pattern.

The power law fitting data confirmed that all the sample groups had similar μ'_s. All the samples had close amplitude c_1 values; c_2 values decreased for darker skins, but they were still close.

Melanin is the main light-absorbing chromophore in the ◀ AU7 visible range and produces the skin pigmentation; its absorbance decreases from 500 to 900 nm. Samples in group 1, with the highest ITA values, had the lowest μ_a, but absorption gradually increased for sample groups with lower ITA values (darker samples). This was expected because the higher the melanin concentration, the proportionately higher the absorption coefficient.[23]

The bands at 540 and 575 nm correspond to oxyhemoglobin bands,[24] whereas the bands at 970 and 1200 nm refer to water bands.[7,8,25] Our results strongly indicated that these bands did not change according to the ITA values. At 1212 nm, the absorption band may overlap due to fat residues,[26] but low concentrations of these residues were present in the samples.

Some authors[14] correlate the skin color by using CIE-LAB. The a^* axis is proportional to the hemoglobin concentration in the blood. This result is expected because the a^* scale indicates skin redness. ITA uses only parameters L^* and b^* to generate its values, so the presence of hemoglobin ◀ AU8 had some impact on our results.

Nevertheless, in in vivo samples, the presence of hemoglobin may provide more information and should be taken into consideration. Water is also very abundant in biological samples. It is transparent in the visible range, but absorbs in the infrared region, so it does not change the colorimetric evaluation proposed herein.

Groups 1 and 2, with ITA values of 32.7° and 29.0°, respectively, had μ_a values similar to previously published

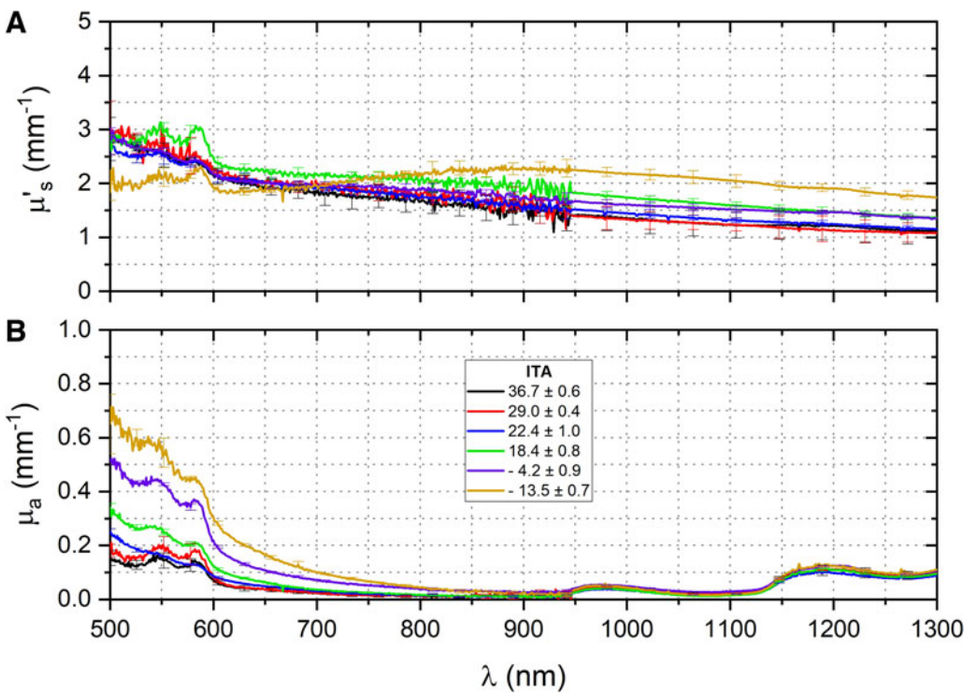

FIG. 2. Optical **(A)** reduced scattering (μ'_s) and **(B)** absorption (μ_a) coefficients of the human tissue groups labeled by ITA values. μ'_s shows a decreasing pattern through wavelengths for all the samples, but the darker sample in group 6 behaves abnormally. μ_a increases when ITA values decrease in the visible range; however, it does not change significantly AU16 ▶ in the NIR range. NIR.

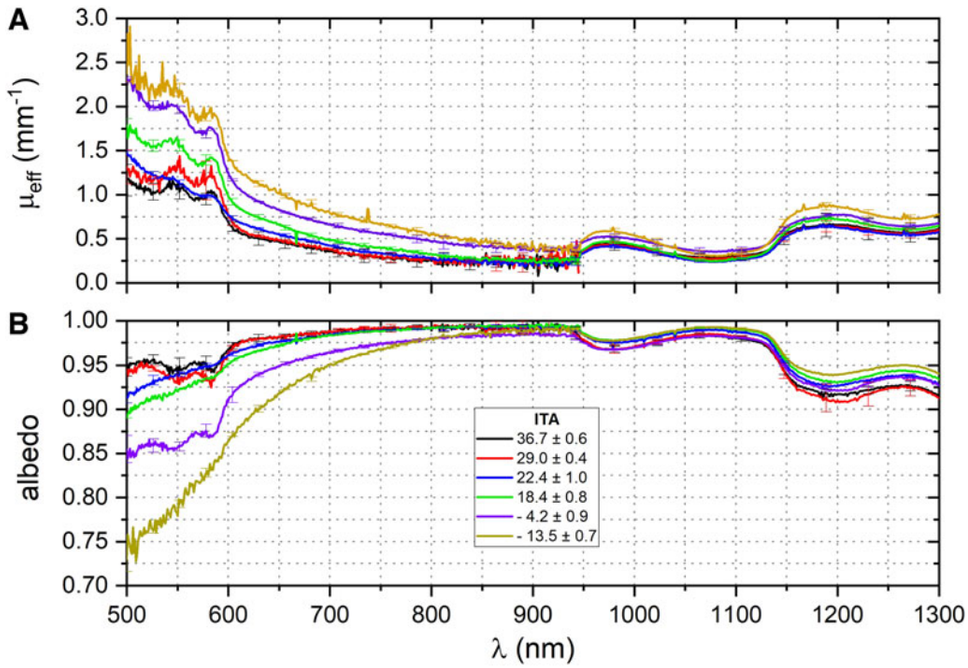

FIG. 3. Skin **(A)** effective attenuation coefficient (μ_{eff}) and **(B)** albedo (a). μ_{eff} increases when ITA decreases, and the inverse is observed for albedo. Prahl indicated that lower albedo ($a > 0.85$) increases the chances of not converging with the IAD algorithm.[20] IAD, inverse adding–doubling.

values[6–8,24,26] obtained for lighter samples. Differences in μ_a values presented here compared with the literature values could be related to (1) the storage time,[10] given that we used fresh samples within 3 h after surgery; (2) the part of the body from which the sample was collected, given that we only analyzed female abdomen tissue; and (3) the local pigmentation variation due to biological individuality.

Comparison with dark skin samples in the literature was not possible because we did not find any study that directly correlated μ_a and μ'_s values of type IV, V, and VI skin with the $L^*a^*b^*$ and ITA color scales. Nevertheless, we found a study with $L^*a^*b^*$ and Fitzpatrick scales for phototypes I, II, III, and IV, which indicated higher absorbance correlation for darker skin.[27]

We observed lower standard deviations in the absorption coefficients of all the samples from the same group. This was expected because the melanin concentration in samples from the same group should be similar.[16] However, for μ'_s, the standard deviation was relatively larger, which was probably related to the donor's age,[12] but not the ITA itself.

Table 2. Power Law Parameters c_1 and c_2 of the Reduced Scattering Coefficients of Our Experimental Skin Data

Group	c_1	c_2	R^2
1	2.60 ± 0.01	0.95 ± 0.01	0.96
2	2.82 ± 0.01	1.03 ± 0.01	0.96
3	2.56 ± 0.01	0.83 ± 0.01	0.99
4	2.76 ± 0.01	0.68 ± 0.01	0.95
5	2.54 ± 0.01	0.67 ± 0.01	0.93
6		Disregarded	

The R-squared (R^2) parameter is also presented to ensure fit.

Effective attenuation, albedo, and depth penetration

By using experimental absorption and reduced scattering from Fig. 2 in Equations (5) and (7), we computed the effective attenuation and albedo of the skin samples (Fig. 3).

The effective attenuation coefficient combines scattering and absorption, so it is an asset for estimating how light would be effectively attenuated when interacting with the tissue.[28] This coefficient can also indicate how opaque the medium can be. This coefficient has a similar pattern to the absorption coefficient, but higher values, and it gradually increases for darker skins (lower ITA values) in the visible range.

Figure 3B shows the albedo of the six skin groups. Between 500 and 600 nm, the albedo had the lowest value and it became even lower for darker skins, ITA = −13.5°, for instance. In the NIR range, the albedo did not change significantly for different sample groups. Although the albedo does not carry crucial information for medical applications, it is relevant in optical analysis.

Algorithms that derive from the transport equation, such as the IAD, and Monte Carlo simulations that use the radiative transport equation assume that the scattering coefficient of the sample is much higher than its absorption, and the albedo indicates the amount of light scattered compared with total attenuation ($\mu_a + \mu'_s$). ◀AU9

Our results suggested that much darker samples, such as group 6, may not be suitably characterized in the visible region through this methodology, as can be seen in the case

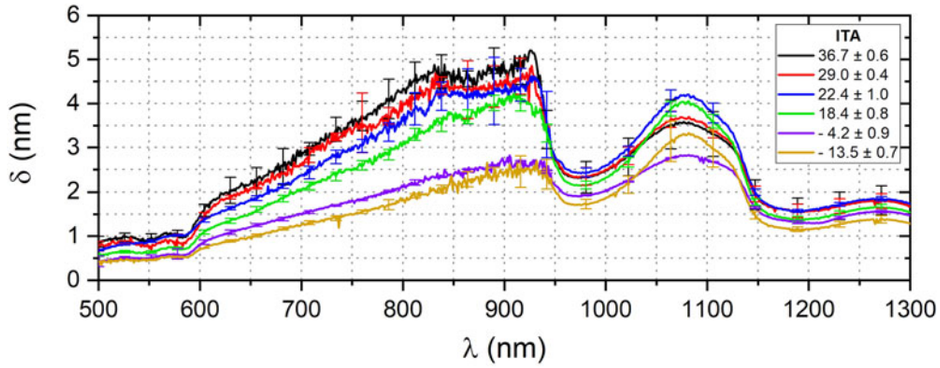

FIG. 4. Human skin depth penetration and their ITA response. Higher ITA values have deeper light penetration, while penetration decreases for lower ITA values.

of μ'_s in Fig. 2A, which showed a lower scattering coefficient for this sample in the visible range, but high values for further wavelengths.

The inverse of effective attenuation ($1/\mu_{\text{eff}}$) refers to optical depth penetration[29]; δ indicates how deep light can propagate in human tissue until its initial intensity is reduced to $1/e$ ($\sim$36%). Figure 4 shows the experimental depth penetration of the six sample groups.

We observed two high-penetration regions. The first ranged from 600 to 900 nm and the second ranged between 1050 and 1100 nm. Both regions are known as first and second therapeutic windows, respectively, and are useful in optical therapies such as PDT.[2,30]

Light penetration was higher in the first therapeutic window region and decreased greatly for darker skins—their maximum depth was close to 5.2 mm for ITA = 32.66°, 4.9 mm for ITA = 29.05°, 4.6 mm for ITA = 22.42°, 4.2 mm for ITA = 18.36°, 2.8 mm for ITA = −4.15°, and 2.7 mm for ITA = −13.45°. Bashkatov et al.[8] also reported similar light skin values for Caucasian skin, with maximum penetration depth close to 4.5 mm in the first therapeutic window.

The region with the lowest optical penetration in the visible range lay from 500 to 600 nm, which was due to melanin absorption with the contribution of hemoglobin bands. In the NIR region, there were two sites of low penetration due to the water bands.

Conclusions

We performed an optical characterization of fresh, ex vivo abdominal skin samples. Through the power law coefficient, we observed that the scattering coefficients of the skin groups are similar and do not change with ITA. The absorption and effective attenuation coefficients increase with decreasing ITA, and the inverse is true for albedo and depth penetration. These results are only valid in the visible region because ITA is a classification based on colorimetric parameters.

Our findings indicate the importance of considering skin color in optical analysis, especially for the design of photonic treatments and devices.

Acknowledgments

The authors thank Cynthia Maria de Campos Prado Manso for linguistic advice.

Authors' Contributions

All the authors made significant contributions to the manuscript. P.S.C. was the surgeon responsible for acquiring all the human tissue samples. C.E.G. was responsible for tissue collection, transportation, cleaning, and disposal. L.B.d.C.J. performed the optical measurements and characterization. L.B. and R.R.d.J.G. supervised this work and made important intellectual contributions. All the authors approved the final version of the manuscript.

Ethics Approval

All the procedures were performed according to ethical standards and approved by the Ethics Committee (ethical appreciation certificate 0630218.2.0000.5440 and approval number 3.275.034).

Author Disclosure Statement

No competing financial interests exist.

Funding Information

This study was partly funded by Coordenação de Aperfeiçoamento de Pessoal de Nível Superior—Brasil (CAPES)—Finance Code 001 and also supported by Fundação de Amparo à Pesquisa do Estado de São Paulo—FAPESP (Grant Nos. 2017/25923-5, 2013/07276-1, and 2018/14955-6).

References

1. Kent KM, Graber EM. Laser tattoo removal: A review. Dermatol Surg 1992;38(1):1–13.
2. Bjordal JM, Couppé C, Chow RT, et al. A systematic review of low-level laser therapy with location-specific doses for pain from chronic joint disorders. Aust J Physiother 2003;49(2):107–116.
3. Sjoding MW, Dickson RP, Iwashyna TJ, et al. Racial bias in pulse oximetry measurement. N Engl J Med 2020; 383(25):2477–2478.
4. Bergmann F, Foschum F, Marzel L, et al. Ex vivo determination of broadband absorption and effective scattering coefficients of porcine tissue. Photonics 2021;8(9):1–19.
5. Prahl SA, van Gemert MJC, Welch AJ. Determining the optical properties of turbid media by using the adding-doubling method. Appl Opt 1993;32(4):559–568.

6. Chan EK, Sorg B, Protsenko D, et al. Effects of compression on soft tissue optical properties. IEEE J Sel Top Quantum Electron 1996;2(4):943–950.
7. Simpson CR, Kohl M, Essenpreis M, et al. Near-infrared optical properties of ex vivo human skin and subcutaneous tissues measured using the Monte Carlo inversion technique. Phys Med Biol 1998;43(9):2465–2478.
8. Bashkatov AN, Genina EA, Kochubey VI, et al. Optical properties of human skin, subcutaneous and mucous tissues in the wavelength range from 400 to 2000 nm. J Phys D Appl Phys 2005;35(15):2543–2555.
9. Salomatina E, Jiang B, Novak J, et al. Optical properties of normal and cancerous human skin in the visible and near-infrared spectral range. J Biomed Opt 2006;11(6):1–8.
10. Genina EA, Bashkatov AN, Kochubey VI, et al. Effect of storage conditions of skin samples on their optical characteristics. Opt Spectrosc 2009;107(6):934–938.
11. Dubin CE, Kimmel GW, Hashim PW, et al. Objective evaluation of skin sensitivity across Fitzpatrick skin types. J Drugs Dermatol 2020;19(7):699–701.
12. Calin MA, Parasca SV. In vivo study of age-related changes in the optical properties of the skin. Lasers Med Sci 2010; 25(2):269–274.
13. Zonios G, Dimou A, Carrara M, et al. In vivo optical properties of melanocytic skin lesions: common nevi, dysplastic nevi and malignant melanoma. Photochem Photobiol 2010;86(1):236–240.
14. Huang WS, Wang YW, Hung KC, et al. High correlation between skin color based on CIELAB color space, epidermal melanocyte ratio, and melanocyte melanin content. PeerJ 2018;24(6):1–17.
15. Chardon A, Cretois I, Hourseau C. Skin colour typology and suntanning pathways. Int J Cosmet Sci1991;13(4):191–208.
16. Bino SD, Bernerd F. Variations in skin colour and the biological consequences of ultraviolet radiation exposure. Br J Dermatol 2013;169(3):33–40.
17. Zonios G, Bykowski J, Kollias N. Skin melanin, hemoglobin, and light scattering properties can be quantitatively assessed in vivo using diffuse spectroscopy. J Invest Dermatol 2001;117(6):1452–1457.
18. Osto M, Hamzavi IH, Lim HW, et al. Individual typology angle and Fitzpatrick skin phototypes are not equivalent in photodermatology. Photochem Photobiol 2022;98(1):127–129.
19. Cruz Junior LB, Bachmann L. Manufacture and characterization of a 3D-printed integrating sphere. Instrum Sci Technol 2020;49(3):276–287.
20. Prahl SA. Everything I Think You Should Know About Inverse Adding-Doubling. Oregon Med Laser Center; 2011. ◀AU12
21. Wu Y, Tanaka T, Akimoto M. Utilization of individual typology angles (ITA) and Hue angle in measurement of skin color images. Bioimages 2020;28:1–8.
22. Alaluf S, Atkins D, Barret K, et al. The impact of epidermal melanin on objective measurements of human skin colour. Pigment Cell Res 2002;15(2):119–126.
23. Madkhali N, Alqahtani HR, Al-Terary S, et al. Control of optical absorption and fluorescence spectroscopies of natural melanin at different solution concentrations. Opt Quantum Electron2019;51(227):1–13.
24. Lister T, Wright PA, Chappell PH. Optical properties of human skin. J Biomed Opt 2012;17(9):1–15.
25. Troy TL, Thennadil SN. Optical properties of human skin in the near infrared wavelength range of 1000 to 2200 nm. J Biomed Opt2001;6(2):167–176.
26. Lauridsen RK, Everland H, Nielsen LF, et al. Exploratory multivariate spectroscopic study on human skin. Skin Res Technol 2003;9(2):137–146.
27. Reis F, Kapoustina V, Kron A, et al. Estimation of skin phototypes with optical parameters: an experimental study using newly developed fibre optic detection device. Int J Cosmet Sci 2013;35(1):50–56.
28. Fishkin JB, Gratton E. Propagation of photon-density waves in strongly scattering media containing an absorbing semi-infinite plane bounded by a straight edge. J Opt Soc Am A 1993;10(1):127–140.
29. Tuchin B. Tissue Optics, Light Scattering Methods and Instruments for Medical Diagnosis. SPIE Press; 2015.
30. Ablon G. Phototherapy with light emitting diodes: Treating a broad range of medical and aesthetic conditions in dermatology. J Clin Aesthet Dermatol 2018;11(2):21–27.

Address correspondence to: ◀AU13
Luismar Barbosa da Cruz Junior ◀AU14
Laboratory of Phobiophysics
Department of Physics
University of São Paulo
Ribeirão Preto
Brazil

E-mail: luismar@usp.br

Received: September 30, 2022.
Accepted after revision: February 16, 2023.
Published online:

AUTHOR QUERY FOR PHOTOB-2022-0111-VER9-DACRUZ_1P

AU1: Please identify (highlight or circle) all authors' surnames for accurate indexing citations.
AU2: Please mention the authors' degree abbreviations (e.g., MS, MD, PhD).
AU3: Please check the word ''Phobiophysics.''
AU4: The Clinical Trial Registration number, if applicable, should be included at the end of the abstract.
AU5: Please expand 3D.
AU6: Please define ''NIR.''
AU7: Please check if the edits made in the sentence ''Melanin is the main light-absorbing chromophore in the visible range and produces the skin pigmentation'' are OK.
AU8: Please check if the edits made in the sentence ''so the presence of hemoglobin had some impact on our results.'' are OK.
AU9: Please check if the edits made in the sentence ''Algorithms that derive from the transport equation, such as the IAD, and Monte Carlo simulations that use the radiative transport equation assume that the scattering coefficient of the sample is much higher than its absorption, and the albedo indicates the amount of light scattered compared with total attenuation ($\mu_a + \mu'_s$).'' are OK.
AU10: Please expand ''PDT.''
AU11: Refs. 21–30 have been renumbered for sequential order of citation in the text and list. Please check.
AU12: In Refs. 20 and 29, please mention the location of the publisher.
AU13: Please mention the degree abbreviation (e.g., MS, MD, PhD) of the corresponding author.
AU14: Please check the word ''Phobiophysics.''
AU15: Please check whether ITA values should be written as mean (SD) values with degree symbol.
AU16: Please define ''NIR.''
AU17: Author Disclosure correct? If not, amend as needed.